Lateral Diffusion of Membrane Proteins in the Presence of Static and Dynamic Corrals: Suggestions for Appropriate Observables

Frank L. H. Brown, David M. Leitner, J. Andrew McCammon, and Kent R. Wilson
Department of Chemistry and Biochemistry, University of California, San Diego, La Jolla, California 92093-0339 USA

ABSTRACT We consider the possibility of inferring the nature of cytoskeletal interaction with transmembrane proteins via optical experiments such as single-particle tracking (SPT) and near-field scanning optical microscopy (NSOM). In particular, we demonstrate that it may be possible to differentiate between static and dynamic barriers to diffusion by examining the time-dependent variance and higher moments of protein population inside cytoskeletal "corrals." Simulations modeling Band 3 diffusion on the surface of erythrocytes provide a concrete demonstration that these statistical tools might prove useful in the study of biological systems.

INTRODUCTION

One commonly studied property of membrane-associated proteins is the proteins' mobility (or lack thereof) in the plane of the membrane. Membrane protein mobility can have far-reaching effects on cellular functioning (Lauffenburger and Linderman, 1993; Giancotti and Ruoslahti, 1999; Berg and Purcell, 1977). Early models of the plasma membrane, notably the fluid mosaic model (Singer and Nicolson, 1972), postulated that proteins were freely diffusing in the plane of the membrane. More recently, it has become apparent that the true situation is more complicated than that suggested by the fluid mosaic model; proteins associated with the membrane surface must contend with various obstacles as they undergo Brownian motion. Study of the hindered diffusion of membrane proteins thus sheds light on the nature of interactions between proteins and the constituents of the membrane interface where they reside. In turn, knowledge of these interactions gives workers a more complete picture of global cellular functioning.

Revision of the fluid mosaic model to incorporate the effects of inhomogeneities in and near the plasma membrane is an active area of research (Jacobson et al., 1995; Edidin, 1990). Although a complete understanding of all of the physical, chemical, and biological mechanisms at play at the surface of cells is still lacking, there exists strong evidence that the cytoskeleton just below the membrane plays a central role in controlling the mobility of membrane proteins in a variety of cells, such as epithelial, nerve, and red blood cells (Fleming, 1987; Saxton, 1990b; Saxton and Jacobson, 1997; Winckler et al., 1999). Erythrocytes, with their unusually dense network of cytoskeletal elements, have been particularly well studied in this context (Cherry, 1979; Schindler et al., 1980; Sheetz et al., 1980; Koppel et al., 1981; Sheetz, 1983), leading to the formulation of the "matrix" (Sheetz, 1983) or "skeleton fence" model for hindered protein transport, in which transmembrane proteins are effectively corralled by a "fence" of cytoskeleton just beneath the membrane. Infrequent jumps over or through the cytoskeletal fence allow proteins to explore the surface of the cell, albeit much more slowly than predicted by the fluid mosaic model (see Fig. 1). Numerous experimental studies have confirmed the predictions of the skeleton fence model in erythrocytes and other cells (Corbett et al., 1994; Tsuji and Ohnishi, 1986; Tsuji et al., 1988; Kusumi and Sako, 1996; Edidin et al., 1991), and theoretical modeling (Saxton, 1989, 1990a,b, 1995; Boal, 1994; Boal and Boey, 1995) has helped in the interpretation of these experiments.

Interestingly, although the basic picture of the skeleton fence model has held up under scrutiny, some detailed aspects of the model have yet to be resolved. For instance, the exact mechanisms proteins use to escape from one corralled region to a neighboring one are unclear. It has been suggested for some time that dynamic reorganization of the matrix itself would lead to jumping between corrals (Sheetz, 1983). Whether this reorganization is predominately associated with spectrin tetramer-dimer dissociation events (Tomishige and Kusumi, 1999; Tomishige, 1997) or with relative motion of the cytoskeleton away from the membrane surface (Boal, 1994; Boal and Boey, 1995) is an unresolved issue. Furthermore, it is unclear that one must invoke a dynamic model for the cytoskeleton to explain experimental results (Saxton, 1995). (Some experimental evidence has been interpreted to suggest that a dynamic cytoskeletal model may be closer to reality than a static picture (Edidin et al., 1991; Tomishige, 1997); however, it is unclear that there is any inconsistency between a static model and these results. To our knowledge, no theoretical treatment has ever shown these experimental results to prove one mechanism over another.) By analogy with Kramer's rate theory for chemical reactions (Hänggi et al., 1990), it would be relatively easy to formulate a picture for bound protein diffusion where corral jumps occur when

Received for publication 9 September 1999 and in final form 28 January 2000.

Address reprint requests to Dr. Frank L. H. Brown, Department of Chemistry and Biochemistry, University of California, San Diego, M/S 0339, La Jolla, CA 92093-0339. Tel.: 858-534-0290; Fax: 858-534-7654; E-mail: flb@chem.ucsd.edu.

0006-3495/00/05/2257/13 $2.00

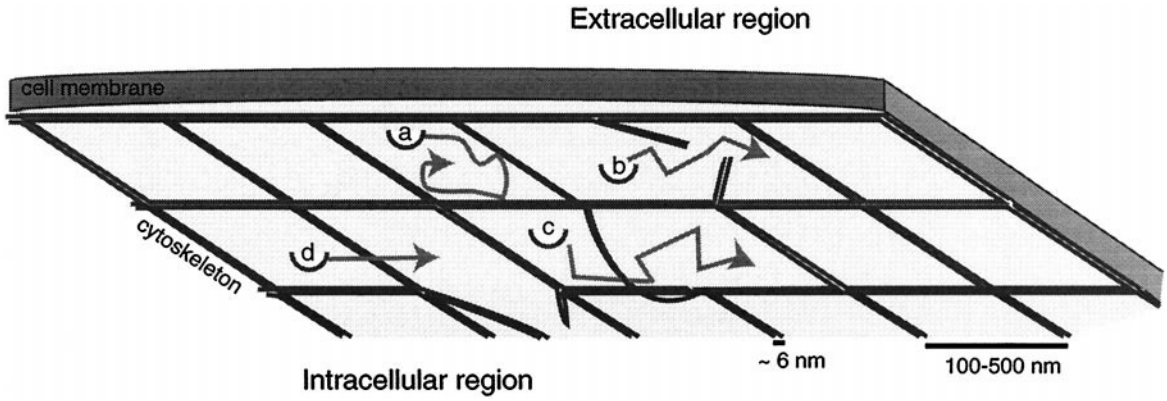

FIGURE 1 Ultraschematic illustration of a mobile transmembrane protein as viewed from under the membrane. The cytoskeleton immediately below the membrane hinders and regulates the transport, confining the protein temporarily to a corral (*a*). Jumps from one corral to another occur slowly and are postulated to result from dynamic reorganization of the cytoskeletal matrix (by dissociation of spectrin tetramers (*b*) or thermal fluctuations in the gap between membrane and skeleton (*c*)) or from infrequent crossing events where the protein is thermally kicked hard enough to force its way over a relatively static cytoskeleton (*d*).

Brownian motion instantaneously "shoves" hard enough to push the protein over a "static" cytoskeletal fence. In this picture, the cytoskeleton and/or membrane still moves, but only when they are shoved away by a protein that happens to be experiencing an especially hard thermal push across the membrane. The static gating picture just described can be thought of in terms of a door that is held shut by a spring. Only when a protein runs into the door with sufficient force does it pass through. This is to be contrasted with a dynamic gating picture in which the door stochastically fluctuates between being open or bolted shut.

In previous work we considered a dynamic gating model where gating was assumed to result from dissociation/association of spectrin tetramers/dimers (Leitner et al., 2000). It was shown that such a model appears to be consistent with the existing experimental data. The question we address in this article is whether it is possible to experimentally infer which of the above-mentioned mechanisms (static or dynamic) is actually occurring in a cell. More specifically, we consider the possibility of differentiating between a static picture such as Saxton's (1995) and a dynamic model for cytoskeletal interference, using noninvasive optical techniques such as single-particle tracking (SPT) and near-field scanning optical microscopy (NSOM). Here we have made the distinction between noninvasive techniques and invasive techniques (such as dragging membrane proteins with laser tweezers) because it is always preferable to observe a system without interfering with it. (Experiments from the Kusumi laboratory (Sako and Kusumi, 1995) suggest that direct manipulation of membrane proteins via laser trapping can lead to deformations in the membrane skeleton. These deformations contain sufficient elastic energy to cause trapped particles to "rebound" when they escape from the trap.) When inferences are made about how a complex system would behave when left alone, on the basis of measurements conducted with a significant perturbation present, there is always the possibility of drawing false conclusions.

We will show that it is possible, in theory, to differentiate between these two pictures. The basic premise is that while a fluorescence recovery after photobleaching (FRAP) recovery curve (averaged over many individual experiments) or similar averaged observables may not provide a clue to the corralling mechanism, there is information contained in the variance and higher moments of the experimental data that is capable of making the distinction. (Throughout this paper we will be referring to FRAP, even when the experiments we describe require looking at length scales inaccessible to FRAP in its conventional form. In these cases, we use FRAP to describe any experiment where a depleted region of proteins is observed in the recovery process. SPT and NSOM are possible experimental realizations of our generic FRAP thought experiment.)

The organization of this paper is as follows. In the next section we present a simple, analytically solvable model that qualitatively captures the behavior just described, namely that higher order moments in the experimental data provide a means of discriminating between static and dynamic cytoskeletal interference pictures. In the third section we present simulation results for Band 3 diffusion in erythrocytes that corroborate the picture established in the second section. In the fourth and fifth sections we discuss our results and conclude.

THEORETICAL MOTIVATION

Before proceeding with a statistical discussion, it is worthwhile to qualitatively consider just what it is we hope to statistically quantify. Suppose we can directly observe a

single corral on the surface of the cell and further suppose that we have labeled the proteins within this corral so that they are observable (proteins in neighboring corrals are unlabeled or have been bleached). If the proteins are numerous enough to simulate a continuous concentration of labels, as opposed to a collection of just a few individually labeled proteins, then we imagine that the concentration of labeled proteins within the corral will decay in time with some characteristic shape indicative of the nature of the cytoskeletal gating mechanism. Suppose, for instance, that the static gating picture holds. Then the probability that individual proteins will escape at any time remains constant and the decay curve will appear smooth. If, however, gating is controlled by an open-closed mechanism (such as spectrin tetramer-dimer equilibrium), then proteins will only be able to escape when the gate is open, and we will observe a staircase (see Fig. 2). It is critical to realize that this staircase will not persist when we average over a number of experiments. The opening and closing of the gates is governed by rate equations of the form

$$\dot{P}_o(t) = -W_c P_o(t) + W_o P_c(t)$$

$$\dot{P}_c(t) = W_c P_o(t) + -W_o P_c(t), \qquad (1)$$

where $P_0(t)$ ($P_c(t)$) is the probability that the gate is open (closed), and W_c (W_0) is the closing (opening) rate. The gate's behavior is not deterministic (a gate that begins open has a probability of staying open for some time interval, but could also close), so that although each experiment will have a staircase shape, the heights and lengths of each step will vary from one experiment to another. When averaging over individual experiments is performed we will obtain a smooth decay curve, and indeed, with a proper choice of parameters in a suitable model, we can imagine obtaining an averaged curve that is identical to that which would be obtained from a static model. A dynamic gating picture leads to concentration versus time profiles with significant variation from corral to corral, whereas a static picture predicts profiles for which the average is the same as that for any individual experiment. Of course, this picture will break down when we have a limited number of proteins or an inhomogeneous membrane surface or any other complication, and this is why it is helpful to think in terms of the variance of the protein population as discussed below.

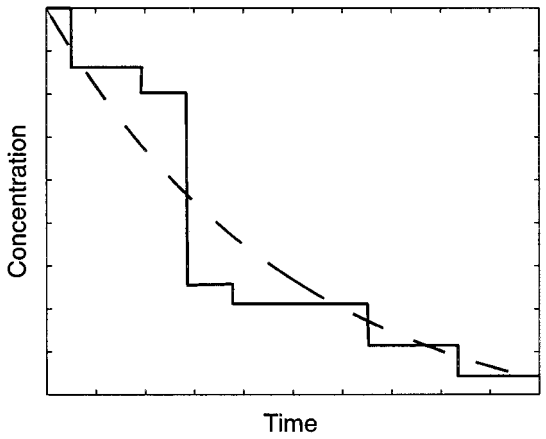

FIGURE 2 Hypothetical concentration versus time plots for labeled proteins within a corral. At zero time we begin with a nonequilibrium distribution of labeled proteins found only inside the corral. It is assumed that there are enough proteins to simulate a continuous concentration within the corral and that a corral with a permanently open gate would exhibit a nearly vertical decrease to zero concentration on this time scale. The dashed line represents the case where a static barrier to diffusion exists at the edge of the corral, and the solid line the case for an open-closed gating mechanism. These curves represent profiles for a single experiment. Averaging over multiple experiments would not affect the dashed curve, but would cause the solid line to smooth (approaching the dashed curve if the gating parameters are chosen appropriately).

We discussed, in the preceding paragraph, the fact that a dynamic gating model will give rise to "significant variation" among individual experiments. If we prepare 100 identical distributions of proteins within a corral, the stochastic nature of the fluctuating gate will guarantee 100 different concentration versus time profiles such as the staircase in Fig. 2. A mathematically meaningful way to quantify this variation is to look at the variance in the number of proteins within the corral as a function of time:

$$\overline{(N(t) - \overline{N(t)})^2} = \overline{N(t)^2} - \overline{N(t)}^2, \qquad (2)$$

where $N(t)$ denotes the time-dependent number of proteins, and the horizontal bars refer to averaging over all possible stochastic trajectories for the gate and all possible diffusive motions for the proteins. In this language $\overline{N(t)}$ is the average time-dependent number of proteins within the corral and will be a smooth curve much like the dashed line of Fig. 2. One need not stop with the variance. Higher order single time moments as well as multiple time correlation functions can shed further light upon the stochastic process of protein depopulation of the corral. (A 10-time correlation, for example, looks like $\overline{N(t_1)N(t_2)\ldots N(t_{10})}$.) In fact, the complete set of correlation functions to all orders serves to completely specify a stochastic process (van Kampen, 1992). In practice this statement is more formal than useful, but it does give us hope that we may be able to differentiate between different gating models by examining a finite number of moments and correlation functions. In the current work we concentrate on distinguishing open-closed gating from a static gating picture. We find that the variance is able to distinguish between these two pictures for sufficiently idealized experiments. Under less than ideal circumstances it is harder to differentiate between the two models.

To rigorously study the statistical behavior of $N(t)$ for a finite number of proteins requires careful consideration of the stochastic behavior associated with Brownian motion as well as any nondeterministic behavior affiliated with the gating process. This is a question we will pursue via simu-

lation in the following section. To get a feel for the physics underlying these simulations we present the following simplified model, which is useful because it is able to qualitatively reproduce some of the trends observed in our simulations and because the model is simple enough to allow for an analytical solution and physical interpretation. The primary assumption of the model is that we may disregard the position of the proteins relative to the gate, categorizing proteins as either "inside" or "outside" the corral and that interconversion between these two flavors of protein is governed by rate processes while the gate is in a set configuration. By "rate process" we simply mean that the waiting time distribution (van Kampen, 1992), $w(t; \mu)$, associated with, for instance, the conversion of an "inside" protein to an "outside" protein in time t, is given by

$$w(t; \mu) = \mu e^{-\mu t}. \tag{3}$$

This waiting time distribution just tells us that a concentration of "inside" proteins will exponentially decay away (with rate constant μ) and that a specific one of these proteins will leave at or after time t with probability $e^{-\mu t}$. Furthermore, we assume the proteins outside the corral to be in a constant state of equilibrium, i.e., that the number of proteins entering or leaving the corral does not affect the bath of proteins outside the corral. In our previous examples this approximation translates to a constant state of zero proteins outside the corral.

In a previous study (Leitner et al., 2000), we found the rate process assumption to be valid for calculating $\overline{N(t)}$ in corrals parameterized to mimic typical cellular environments. Extending this assumption beyond the first moment, $\overline{N(t)}$, to the calculation of higher moments seems a natural thing to try. Under the set of approximations just described we analytically obtain, for the average population and variance of proteins in a *static* corral (see Appendix),

$$\overline{N(t)} = (N(0) - \langle N\rangle)e^{-\mu t} + \langle N\rangle$$

$$\overline{N(t)^2} - \overline{N(t)}^2 = N(0)e^{-\mu t}(1 - e^{-\mu t}) + \langle N\rangle(1 - e^{-\mu t}), \tag{4}$$

where $N(0)$ is the initial number of proteins found in the corral, $\langle N\rangle$ is the average number of proteins within the corral once equilibrium is established, and μ is the rate constant for decay out of the corral defined by Eqs. 3 and A1. The numerical value of this constant is obtained in a manner described in our previous work (Leitner et al., 2000). Analogous quantities for a dynamically gated two-state corral take the form (see Appendix)

$$\overline{N(t)} = (N(0) - \langle N\rangle)\mathcal{W}_1(t) + \langle N\rangle \tag{5}$$

$$\overline{N(t)^2} - \overline{N(t)}^2 = N(0)(\mathcal{W}_1 - \mathcal{W}_2) + \langle N\rangle(1 - \mathcal{W}_1) + (N(0) - \langle N\rangle)^2(\mathcal{W}_2 - \mathcal{W}_1^2)$$

$$\mathcal{W}_1(t) \equiv \langle e^{-\int_0 \mu(\tau)d\tau}\rangle_T$$

$$\mathcal{W}_2(t) \equiv \langle e^{-2\int_0 \mu(\tau)d\tau}\rangle_T,$$

where the functions $\mathcal{W}_1(t)$ and $\mathcal{W}_2(t)$ are the generalizations of the exponentials $e^{-\mu t}$ and $e^{-2\mu t}$ from Eq. 4 when the gating becomes dynamic and the rate constants accordingly assume a time dependence (see the Appendix for an explanation and explicit formulae for computation). For two-state gating these functions both exhibit simple biexponential decay.

We show in Fig. 3 a direct comparison between simulation and theory for the case of a dynamic corral with some different gating parameters. The behavior we see is typical in that we get good qualitative representation of trends, but the plots are quantitatively off. We do not expect our simplified model to perform perfectly because of the as-

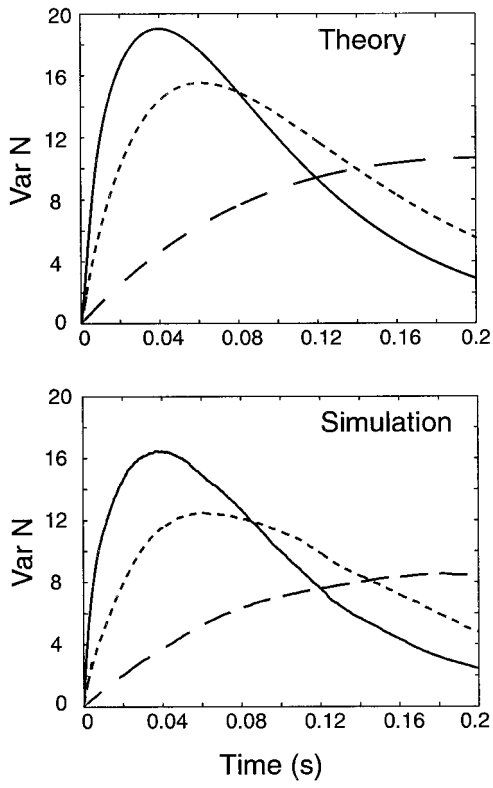

FIGURE 3 Plots of the variance versus time for inverse FRAP experiments, i.e., where an initial nonequilibrium distribution of proteins within the observation region proceeds to decay away, with three different sets of dynamic gating parameters. The dynamic gate fluctuates between being completely open and completely closed. The simulated curves were obtained from Monte Carlo runs, as detailed in our previous work (Leitner et al., 2000), and the theoretical curves from Eq. 5. In each simulation, the corral is a square of side length 128 nm initially occupied by 10 proteins ($N(0) = 10$), diffusing with constant $D = 0.5\ \mu m^2\ s^{-1}$. The equilibrium value for protein occupation, $\langle N\rangle$, is zero. The gating rate constants are $W_0 = 20\ s^{-1}$ and $W_c = 80\ s^{-1}$ (*solid line*); $W_0 = 20\ s^{-1}$ and $W_c = 320\ s^{-1}$ (*dotted line*); $W_0 = 10\ s^{-1}$ and $W_c = 1280\ s^{-1}$ (*dashed line*). These particular parameters, while distantly related to Band 3 diffusion in erythrocytes, are only intended to be suggestive.

sumptions involved. Our equations (Eqs. 4 and 5) are exact for the problem of decay and/or growth of a set of particles governed by static and dynamic rate constants. By looking at solutions to this model problem we make some observations that should approximately hold for our skeleton fence model for protein diffusion. Insight gained in this manner has motivated the numerical simulations found in the next section (Simulations).

By inspection of Eq. 4 we see that when $N(0) = 0$ the variance equals the average population for a statically gated corral. The case $N(0) = 0$ corresponds to a FRAP experiment where the bleached region corresponds exactly to a single corral. One could envision an experimental realization of this initial condition by following multiple particles in a SPT experiment with all particles removed from the corral to start with. In any case, the theoretical implication is clear and is not surprising: for a static gate we observe Poisson-like statistics (van Kampen, 1992). For the corresponding dynamic case we do not find that the variance equals the population, and in fact the two can be quite different (Fig. 4). The FRAP-type initial condition is particularly appealing because the variance and population are both zero at zero time, so there is no uncertainty associated with the state of the system when the experiment is begun. We will see in the next section that when there is such an initial certainty it serves to obscure the statistical signatures of the gating process.

Changing the model parameters will change the shapes and time scales of all population and variance curves. It is particularly interesting to consider how changing the number of particles affects the curves. In Fig. 4 we present illustrative FRAP variance curves for different values of $\langle N \rangle$. Larger values of $\langle N \rangle$ correspond to higher densities of proteins at equilibrium. We see that at high values of $\langle N \rangle$, static and dynamic gating give rise to very different variances, whereas at low values the curves are more similar. This trend tells us that if we want to identify gating mechanisms we should look at a system with a high density of proteins. This makes sense because the inherent noisiness of the diffusion process is relatively large for a small number of proteins. (The uncertainty in the path traveled by a particle undergoing Brownian motion is significant, but the evolution of an infinite number of such particles is governed by the diffusion equation, which is completely deterministic.) The inverse experiment (beginning with proteins inside the corral and none outside) shows similar behavior, but with even more pronounced changes with protein density (see Fig. 5). The almost perfect coincidence of the static and dynamic variance curves in Fig. 5 for the one-protein case reflects the fact that we cannot hope to learn about the gating mechanism when we have only a single protein to observe. All we can see is that the protein leaves the corral with some distribution of waiting times, and this information is completely encoded in $\overline{N(t)}$ (which is taken to be identical for the static and dynamic cases). Without at least two proteins present to allow for possible correlations between decay times, there is no additional information that could serve to distinguish gating mechanisms. Distinguishing between mechanisms requires a large statistical pool of proteins to characterize the stochastic process. In the limit of very large $\langle N \rangle$ we are led to the "smooth" versus "staircase" picture from earlier in this section. In this limit, we can

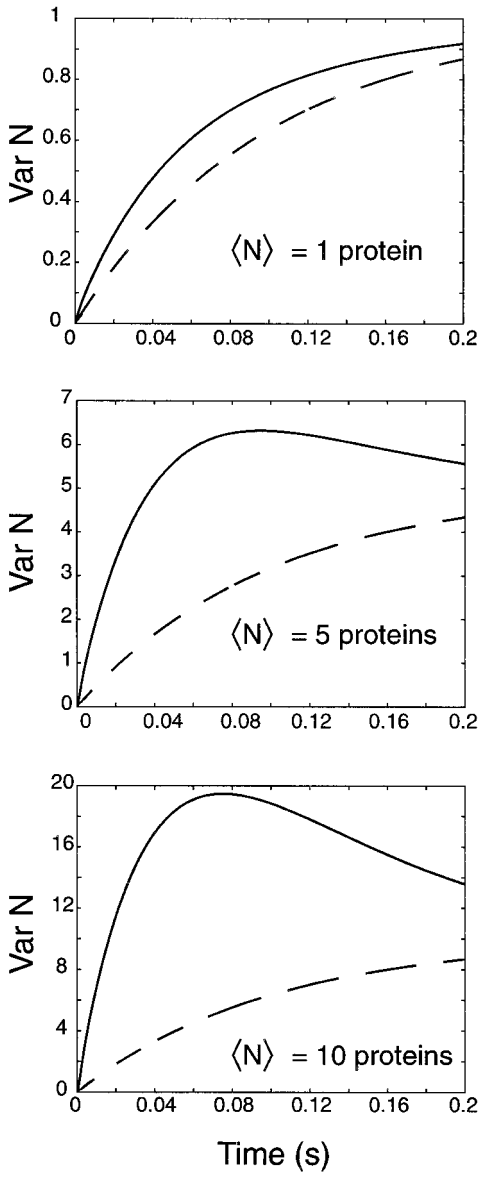

FIGURE 4 Theoretical plots of the variance versus time for FRAP-type experiments with different equilibrium protein populations, $\langle N \rangle$. Except for the equilibrium population, the parameters in each panel are identical: $D = 0.5\ \mu m^2\ s^{-1}$, and the square corral under observation has sides of length 128 nm. The dynamically gated case in each panel (*solid lines*) is specified by gating rates $W_0 = 20\ s^{-1}$ and $W_c = 320\ s^{-1}$, while the transmission probability for the static gating case (*dashed lines*) is taken to ensure matching of the population curves between static and dynamic models. To within the resolution of these plots, the population curves fall on top of the static variance curves.

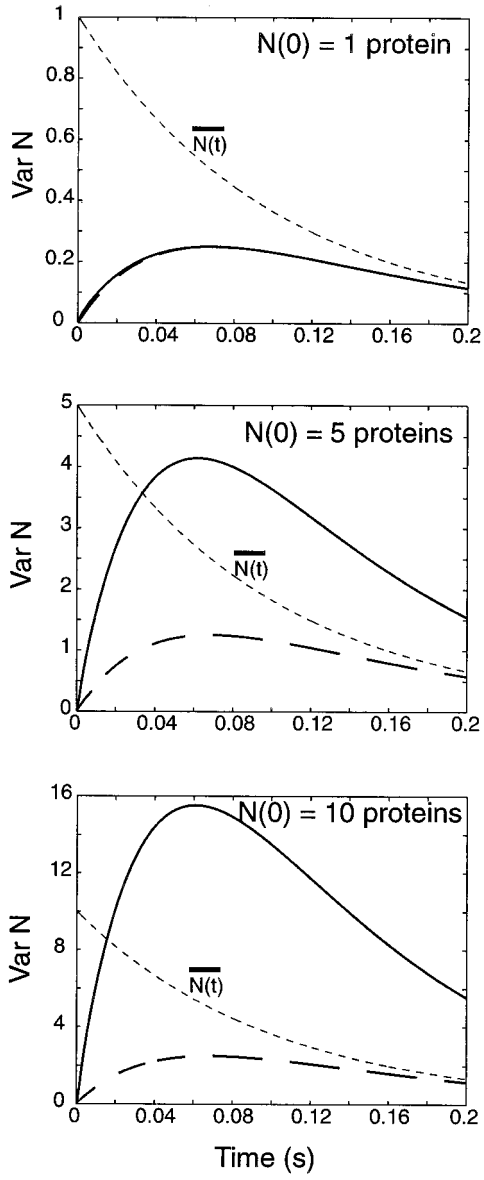

FIGURE 5 Theoretical plots of variance versus time for an inverse FRAP-type experiment (proteins begin localized inside the corral with none outside) with different initial numbers of proteins, $N(0)$. The model parameters are the same as in Fig. 4. Also, as in Fig. 4, the thick solid line is the dynamic case and the thick dashed line is the static case. The population of the corral is given by the thin dotted line for comparison and is the same for both static and dynamic models by construction. Notice that with one protein it would be impossible to distinguish the two models—there must be several proteins to overcome the inherent noisiness of a small number of proteins and observe the effect of the gating mechanism.

distinguish between gating processes by inspection of a single FRAP recovery curve. Cases intermediate between $\langle N \rangle = 1$ and $\langle N \rangle \rightarrow \infty$ will still allow for differentiation of gating mechanisms; however, the statistical signatures of the gate will be obscured by the inherent noisiness of a small number of proteins. This is the regime where our analysis proves useful.

A similar trend is seen if we consider a dynamic corral with multiple gates. Within our simple model, we account for multiple dynamic gates on the same corral by making our opening rate faster (linearly with gate number) while allowing fewer proteins to escape per opening event. More rigorously, if we are worried about more than one gate opening at a time, we can extend the two-state picture to an $M + 1$-state picture, where M is the number of gates. There are then $M + 1$ rates at which proteins can leave, depending upon how many gates are open at a given time. We illustrate this in Fig. 6. Not surprisingly, increasing the number of gates on the corral leads to a decrease in variance. Within the staircase picture, we will have more but smaller steps than we do for a single gate, and this leads to a lowered variance. In the limit of an infinite number of gates, the dynamic and static gating models will become indistinguishable.

We conclude from our simple modeling that it should be possible to distinguish between corral gating mechanisms simply by looking at the higher than first-order moments of protein population within the corral. In particular, it would appear that we will be able to distinguish between two-state dynamic gating mechanisms and static mechanisms by looking at the variance alone (when there are a sufficient number of proteins and a limited number of ways to escape the corral and it is possible to directly observe a single corral region).

SIMULATIONS

The analytical results of the previous section are appealing in their simplicity but were derived with certain approximations. Furthermore, we focused attention on a single corral in a bath of diffusing proteins. This model falls well short of the true situation on a cell membrane where each corral is linked to neighboring corrals via a continuous "matrix" of cytoskeletal barriers. In this section we present a series of simulations performed on a somewhat more realistic model for the cellular surface. This model explicitly includes the Brownian motion behavior of the diffusing proteins as well as the interaction among neighboring corrals. We also investigate the question of observing statistical signatures of the gating mechanism when we are not able to exactly align the observation region with the edges of a corral.

Our model for the cellular surface includes two basic components. The first of these is the diffusive motion of the membrane proteins, which we simulate via a random walk on a two-dimensional square lattice. The cytoskeletal gates are taken, for simplicity, to define a grid of barriers superimposed upon this lattice (see Fig. 7) and comprise the second of our components. For the dynamic gating case, each segment (line between two barrier vertices) is allowed to open and close independently of all other segments. A protein that encounters a closed barrier segment during its random walk is returned to the point it last occupied before hitting the barrier. For the static gating simulations, a pro-

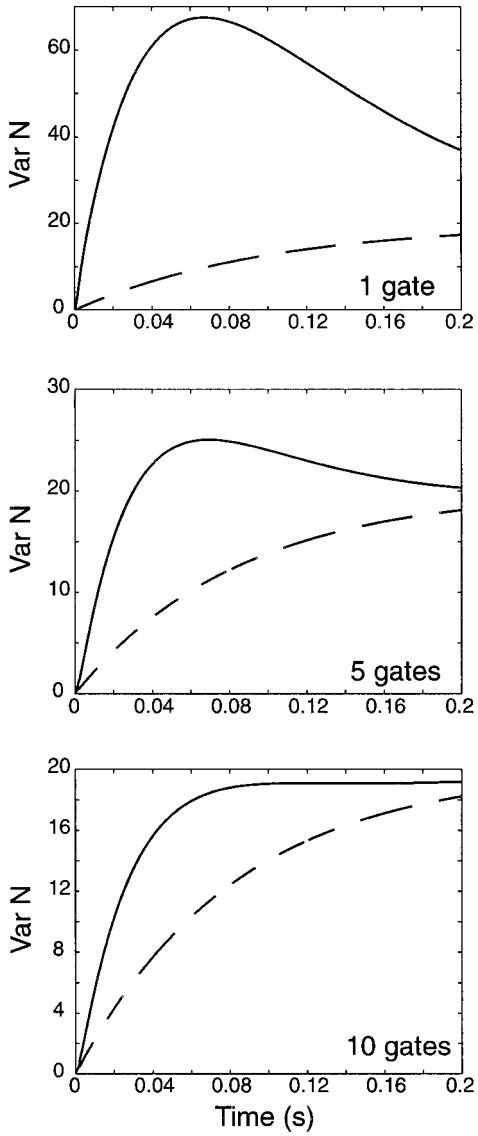

FIGURE 6 Theoretical plots of variance versus time for a FRAP-type experiment with different numbers of gates around the corral. The model parameters are the same as in Fig. 4, with $\langle N \rangle$ always equal to 20. The solid lines are the dynamic model and the dashed line the static model chosen to give agreement between dynamic and static gating population curves (indistinguishable from the *dashed line*). As the number of gates increases ($\langle N \rangle$ constant), the signature of dynamic gating begins to fade relative to the static case.

tein that tries to cross a barrier during its random walk is allowed to cross with a probability P_t or is reflected back to its previous point with probability $1 - P_t$. As we may only simulate a finite lattice of points we impose periodic boundary conditions on our simulation to send proteins that walk off the edge of the simulation to the opposite side. Because our "experimentally observable region" will be taken to be much smaller than the size of our lattice, this periodicity has negligible consequences.

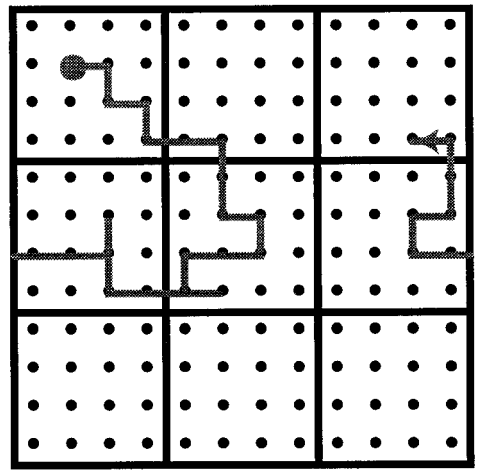

FIGURE 7 Schematic diagram for our model of the membrane surface. A protein (*gray dot*) randomly walks among the lattice points (*black dots*) until it tries to walk through a barrier (*any black line segment*). In the static barrier model the protein will pass through the barrier with probability P_t, or it will stay at the last point it occupied before the barrier was encountered with probability $(1 - P_t)$. In the dynamic barrier model the protein will only pass if that particular barrier happens to be open; otherwise it remains in its previous position. The dynamics of the gates are regulated by Eq. 1. A protein that walks off the edge of the lattice in the simulation is sent to the opposite side.

For concreteness and to establish contact with experiment and our own previous theoretical efforts (Leitner et al., 2000), we have chosen parameters for our simulations to correspond with Band 3 diffusion on the surface of erythrocytes. Our treatment is very approximate, and for this reason we caution the reader against thinking of our results as "red blood cell results." (For example, we have used a uniform square mesh of barriers rather than a heterogeneous triangular one, which would more closely resemble the cytoskeletal network of a true red blood cell. Moreover, the numerical values of many of our parameters are accurate, at best, only to within a factor of ~2 because of experimental ambiguities.) We prefer to classify our simulations as illustrative results, using parameters typical of red blood cells. The set of parameters we have used will be discussed briefly in the next few sentences and is summarized in Table 1. The

TABLE 1 Simulation parameters for Band 3 on erythrocyte membrane

Parameter	Description	Value
L	Corral dimension	140 nm
D	Diffusion constant	0.53 $\mu m^2\ s^{-1}$
N_P	Average number of proteins per corral	33
l	Lattice spacing	7 nm
Δt	Time Step	2.3×10^{-5} s
N_c	Number of corrals	25, 144
W_0	Gate opening rate (dynamic)	14 s^{-1}
W_c	Gate closing rate (dynamic)	4500 s^{-1}
P_t	Transmission probability (static)	1.0×10^{-3}

distance between segments of our barrier grid is taken to be $L = 140$ nm (Tomishige, 1997; Tomishige et al., 1998), so that each corral is a 140 nm $\times$ 140 nm square. Diffusion of Band 3 in the absence of barriers is given by the diffusion constant $D = 0.53\ \mu m^2\ s^{-1}$ (Tomishige, 1997; Tomishige et al., 1998). We divide each corral into a 20 $\times$ 20 grid of points upon which the protein random walk will occur, so that each protein moves 7 nm $\equiv l$ per time step $\Delta t = 2.3 \times 10^{-5}$ s, ensuring adherence to the diffusion equation, $l^2 = 4D\Delta t$. The average number of mobile Band 3 dimers per corral is taken to be $N_p = 33$. (Given that the erythrocyte membrane surface area is $\sim$40 μm^2 (Williams et al., 1990) and it contains 1.2×10^6 Band 3 monomers (Gennis, 1989), we would calculate an average occupation of 84 band 3 dimers per 0.14 μm $\times$ 0.14 μm corral. We have rounded this number down to 50, thus ensuring that any qualitative effects we observe manifest themselves in a conservative fashion. As the mobile fraction of Band 3 is approximately two-thirds of the total found in the cell (Tomishige et al., 1998), we arrive at the stated result.) Our simulations will consist of a group of N_c corrals interconnected in a $\sqrt{N_c} \times \sqrt{N_c}$ array. The results we present will be almost exclusively for $N_c = 25$. For dynamic corralling the opening and closing rates of the gates are given by $W_0 = 14\ s^{-1}$ (Tomishige, 1997) and $W_c = 4500\ s^{-1}$ (Leitner et al., 2000), respectively. For static corralling, we found that the transmission probability of $P_t = 0.001$ gives average population curves that are indistinguishable from the dynamic case, using the rates defined above.

Figs. 8–11 display our simulation results. Although individual details may be found in the captions, we make some general statements here. Each simulation represents a FRAP-type experiment in which the initial condition corresponds to $N(0) = 0$ for the observation region. We arrive at this initial condition by placing $N_p \times N_c$ proteins randomly on our lattice (two proteins may occupy the same lattice point because we assume no protein-protein interaction) and removing from the simulation all proteins within the observation region. The simulation is then allowed to proceed. At each time step every protein is moved one lattice spacing in a randomly determined direction. If a barrier is crossed or a

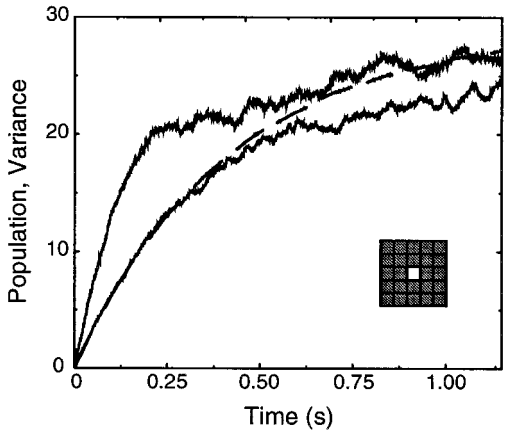

FIGURE 8 Population, $\overline{N(t)}$ (*dashed line*), and variance $\overline{N(t)^2} - \overline{N(t)}^2$ (*solid lines*), versus time for FRAP-type experiments with dynamic and static barriers to diffusion. The population curves are indistinguishable for these two models. The upper solid line is the dynamic gating variance, and the lower solid line the static barrier variance. This simulation was run on a grid of 25 corrals, with the bleached region corresponding to a single corral (see *inset*). Parameters were chosen to simulate Band 3 on an erythrocyte membrane, as shown in Table 1.

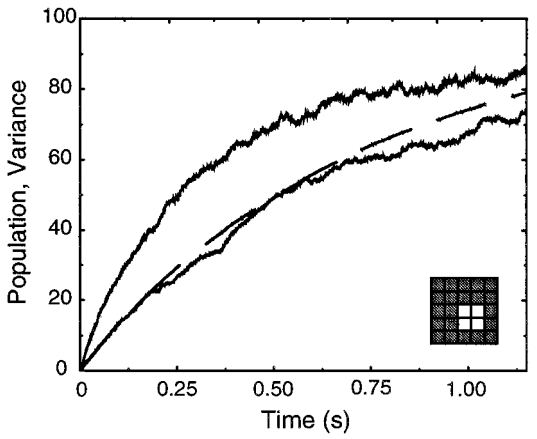

FIGURE 9 Similar to Fig. 8, but with a bleached region corresponding to four corrals (see *inset*). Again, the dashed line represents the population recovery and is the same for both static and dynamic mechanisms. The solid lines correspond to dynamic (*top*) and static (*bottom*) models.

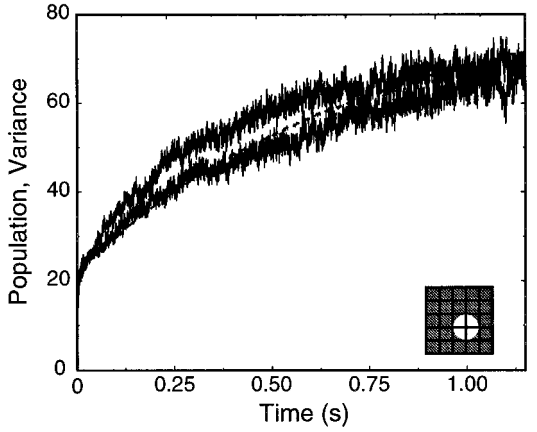

FIGURE 10 Similar to Figs. 8 and 9, but with an observation region consisting of a circle of radius $L = 140$ nm that just fits inside a four-corral square as seen in the inset. The dashed population curve is barely visible here, as it is mostly obscured by the lower (static barrier) variance curve. The rapid rise of all of the curves to $\sim$20 reflects the fact that the initial bleach leaves a number of proteins near the observation region without any barrier to slow their entrance. These proteins rapidly reequilibrate inside the four corrals where the circular observation region lies. The higher noise levels in these curves relative to the previous two figures result from the constant rapid changes in $N(t)$ associated with proteins that pass through no barriers but still enter and leave the observation region. This additional noise is not fully averaged out by looking at only 1000 experiments.

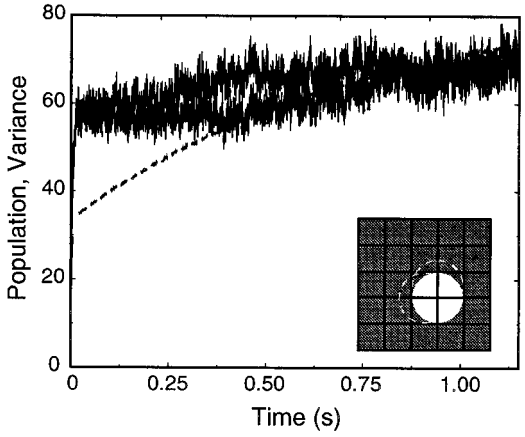

FIGURE 11 Similar to the previous figures, but with a circular observation region (radius = L) that is randomly placed at a different lattice position for each of the 1000 "experiments" over which we average. Our curves here thus represent averaging over not only diffusion and gating statistics, but also the placement of the observation region on the cell membrane. This additional randomness leads to an inherent variance in $N(t)$ for early times as proteins rush into the observation region unhindered by barriers. This "noise" associated with uncertainty about the observation region largely obscures any statistical signatures of the gate mechanism.

protein walks off the edge of the lattice, the move is dealt with in the manner described above. For the dynamic gating case, the status of all of the gates is reevaluated (see Eq. 1) at each time step after the proteins have moved. $N(t)$ was determined for each run by checking to see how many proteins were inside the observation region after each time step. Simulations were run for 50,000 time steps, corresponding to a physical time of 1.15 s. The reported values of $\overline{N(t)}$ and $\overline{N(t)^2} - \overline{N(t)}^2$ were calculated by repeating the above procedure 1000 times and averaging.

It should be clear by looking at our figures that no effort was made to converge our results by increasing our averaging beyond 1000 systems. Our intent is to provide a qualitative demonstration of a general phenomenon. It would be somewhat misleading to give fully converged results when an experiment will almost certainly not be able to approach the statistics necessary to achieve such convergence. Our results mimic what an experimentalist would see if the experiment were repeated 1000 times. Furthermore, the qualitative features we seek from the data, namely to demonstrate the difference between statistical signatures for different mechanisms, are sufficiently apparent when we use 1000 systems. (Repeating the experiment only 100 times results in insufficient statistics to clearly display these signatures.) Our relatively large lattice spacing of $l = 7$ nm deserves comment. The time scale set by this spacing implies a closing rate of approximately once every 10 time steps and an opening rate hundreds of times slower. We do not anticipate inaccuracy in the gating statistics because of this time step, though it could be possible that the behavior of proteins near the gate is affected by this coarse graining. We have observed only very minor changes in preliminary calculations on going from $l = 7$ nm to $l = 7/4$ nm, and certainly no qualitative discrepancies were observed. The spacing we have used is appealing because it is numerically efficient and allows us to ignore any complicated behavior that might be occurring near the cytoskeleton. We have not considered any detailed mechanism for interaction between the cytoskeleton and the proteins that would become important to consider were we to reduce the step size in our simulations. We prefer to consider relatively large length scales and impose a reflecting boundary condition between points that straddle the cytoskeleton. Such neglect of details near the cytoskeleton has been invoked previously (Saxton, 1995; Leitner et al., 2000), and insofar as our work is intended to compare with previous theories (as well as to motivate experiments), we feel justified in this approximation. Saxton (1995) has discussed (although not pursued) the problem of more rigorously dealing with the protein/cytoskeleton interaction, and we refer the interested reader to his work.

The figures we have presented illustrate that the variance can be a probe for distinguishing open-closed gating from a static mechanism in a "realistic" biological system. In the best-case scenarios (Figs. 8 and 9) the early time dynamic variance is significantly different from the early time population, which is not true for a static gating mechanism. It is clear that at short times we may see the gating statistics, even when our observation region encompasses several corrals, as long as the boundaries of the observation region correspond with corral boundaries. When the observation region is not assumed to be perfectly aligned with corral boundaries the differences between the two cases are lessened but persist. We comment further in the following section.

DISCUSSION

The simulations of the preceding section corroborate our findings from the simple analytical models of the second section (Theoretical Motivation). In particular, when the observation is exactly aligned with corral boundaries, it is possible to distinguish between static and dynamic gating mechanisms of the cytoskeleton by examining the time-dependent variance of population within corrals. Experimentally, a worker would collect a series of $N(t)$ FRAP measurements for different observation regions on the cell and average to obtain $\overline{N(t)}$ and $\overline{N(t)^2} - \overline{N(t)}^2$. If the early time behavior of the variance closely follows that of the population, it could be concluded that static barriers are present. Conversely, if the two curves show different behaviors (*i.e., different slopes at early times*), this would be strong evidence for dynamic gating. This picture should hold up even if the dynamic gating is not of the open-closed type, although the differences between population and vari-

ance may be less pronounced for other dynamic corralling models.

Our simulations have focused on the FRAP-type experiment because the time dependence of the population and variance are the same in the static case. Other nonequilibrium experiments beginning with a concentration of proteins within the corral would also yield distinct variance curves, depending on the corralling mechanism, but $\overline{N(t)}$ would bear no resemblance to either variance curve. In such cases, it would be difficult to identify the mechanism from the statistics without actually comparing to simulation. The Poisson-like behavior of variance following the population in time is a clearly identifiable flag that sets FRAP-type measurements apart as a potentially useful technique. One could also envision experiments on equilibrium systems, thus removing the need to bleach out the corral. We have considered such cases, but in our experience nonequilibrium measurements yield the strongest signatures of the gating behavior. Primarily this is because we can specify a particular initial state for the system, so that there is no noise at all in $N(t)$ when the measurement begins. Trying to find an equilibrium observable with an easily identifiable gating signature is difficult because the measurements are obscured everywhere by equilibrium noise similar to the signals in Fig. 11. The statistics of the gating mechanism must be buried in the equilibrium observables, but not so obviously in the low-order moments and especially not when averaging is carried out over a finite number of experiments.

Restriction to the population and variance in this study has been a choice, not only of simplicity, but also of practicality. The noisiness in our simulation results reflects the fact that we averaged each plot over only 1000 experiments; the Monte Carlo procedure has not completely converged, and the convergence gets poorer on going from the population to the variance. This trend will continue to higher order observables as the statistically meaningful combinations of moments will result from the addition and subtraction of terms on the order $N(t)^n$ for nth-order observables. We will need more and more individual runs to converge higher and higher order observables. Although we can achieve this to some extent numerically, experimentalists are limited in the number of measurements they can perform. Our claims that the variance is a useful observable would be meaningless if it took 10^6 experiments to differentiate possible gating mechanisms. We have presented observables that we think are practical and are capable of distinguishing between two models proposed in the literature.

Some features of our simulation results warrant attention. The variance curves in the simulations appear to be reduced in magnitude relative to theory (see Fig. 3), and, in particular, the static curves appear to systematically drop below the population lines at late times. In our rate equation theory (Eq. 4) the static variance and population would exactly coincide. The discrepancy here results from the approximations in our theory. The proteins that enter the bleached region come from neighboring corrals that are not infinite reserves of protein. When a protein enters the bleached corral it is depleted from a neighboring corral, which makes the recovery process a little more deterministic than would be the case for a single huge bath of proteins coupled to the observed corral. For the dynamic gating case we have also invoked the rather severe approximation in our theoretical calculations that all of the proteins within the corral leave with an exponential waiting time distribution. This approximation was motivated by the fact that we can adequately approximate the short time depopulation of an open corral as exponential decay if we are only interested in studying $\overline{N(t)}$ for corrals that are transiently open (Leitner et al., 2000). One possible way to achieve exponential decay of $\overline{N(t)}$ is to impose an exponential waiting time for decay on each protein within the corral, but this approach is not physically motivated and was only chosen to simplify the equations. It should be clear that the proteins within a corral are not all equally likely to leave at a given time, because a protein at the center will be far less likely to escape than one at the edge. This behavior translates to a reduced variance relative to the simple theory of the second section and explains why our simulations show diminished signatures of gating.

Happily, although somewhat smaller in effect than predicted by our simple estimates, gating manifests itself in the variance curves. Also fortunate is the fact that the statistics appear robust with respect to the size of the observation region, as long as the region is taken to coincide with the boundaries of the corral meshwork. Indeed, simulations on somewhat larger regions show very similar statistical signatures of dynamic gating when the observation region is chosen to coincide with the corralling boundaries (unpublished results). Unfortunately, these signatures are markedly reduced when we complicate matters by choosing an observation region that is not aligned with the cytoskeletal meshwork (Figs. 10 and 11). The reason for this is clear and was alluded to in the previous section. Basically we are trying to sort out the "noise" connected with a dynamic gate, which is superimposed on a baseline of noise from the diffusion of the proteins. Our job is made much more difficult when we are forced to contend with additional noise associated with the placement of the observation region. Eventually, it becomes impossible to observe the gating when we can only perform a finite number of experiments. Averaging over more experiments could potentially alleviate this problem, but for severe enough situations (imagine an observation region that is square, with all edges passing through corral centers and the corrals are very large) we will be faced with a hopeless situation. Clearly, the best way to perform the experiments we describe is to perfectly align the observation region with the cytoskeletal meshwork for each measurement. Failing this ideal experiment, it may still be possible to learn about the system if the observation region

closely follows the meshwork (Fig. 10), but severe departures will mask the statistical signatures of the gating mechanism.

CONCLUSION

This work represents an initial theoretical study of how it might be possible to indirectly see the cellular cytoskeleton in motion. The question of whether the cytoskeleton is dynamically interfering with protein motion on the surface of cells or whether its effect is primarily static remains unanswered. We do not advance either hypothesis here, but rather suggest that a dynamic cytoskeleton should influence the motion of membrane proteins in a manner different from that of a static skeleton. Our particular dynamic model (open-closed gating) continues to find support in the recent literature (Tomishige and Kusumi, 1999) and leads to quite different behavior than predicted for a static corralling mechanism. Comparison to other dynamic models (e.g., cytoskeletal diffusion; Boal, 1994; Boal and Boey, 1995) has not been attempted at this point.

Our use of the acronym FRAP should not lead the reader to conclude that the experiments we suggest could easily be carried out using a currently available FRAP apparatus. In fact, the size of most cytoskeletal corrals (generally between 100 and 600 nm across) is less than or comparable to the diffraction limit for light, which precludes a straightforward FRAP measurement of a single corral. It might be possible to get around this problem by looking at a multiple corral region, but our results suggest that this experiment would only be useful if the observation region could be aligned with the cytoskeletal network. As pointed out earlier, our proposed FRAP-type experiment would more easily be carried out with an alternative technology. Particle tracking (Qian et al., 1991; Saxton and Jacobson, 1997) would seem to be an obvious choice and could be extremely powerful if coupled to laser tweezer experiments (Edidin et al., 1991; Kusumi et al., 1998), which could first map out the corral boundaries. Near-field (Levi, 1999) and multiphoton techniques (Squier, personal communication) could also potentially be used to study the phenomenon we have described.

The statistical analysis presented here is very general and is not limited to membrane protein diffusion or even to biological systems. Our theoretical treatment provides an analysis for a finite system of particles interconverting via time-dependent rate processes and could, be applied, perhaps, to systems of chemical interest. Similar theories, utilizing higher statistical moments than the population to differentiate between competing mechanisms, have recently been applied to the field of single-molecule spectroscopy (Wang and Wolynes, 1995). More generally, the classification of a stochastic process by its moments and correlation functions is a standard technique of statistical physics (van Kampen, 1992) that should find many varied applications in biology.

APPENDIX

In this appendix we demonstrate how analytical expressions for various corral observables may be obtained when we approximate the flow of proteins into and out of the corral by rate processes. In particular, we derive expressions for the population, $N(t)$, and variance, $\overline{N^2(t)} - \overline{N(t)}^2$, of proteins within static and dynamic corrals. Expressions for other observables (multiple time correlation functions, higher moments, etc.) may be obtained in a similar (but algebraically messier) fashion.

Static corral

We consider an isolated corral in a "sea" of proteins at thermal equilibrium. This sea of proteins is taken to be infinite and is not influenced by the presence of the corral, in the sense that loss of proteins to the corral and/or gain of proteins from the corral does not change the statistical probability of another gain/loss event occurring. With the additional assumption that we may describe the loss of proteins from the corral and the influx of proteins to the corral as rate processes, the problem becomes analytically tractable. We stress that the rate process assumption is quite adequate for describing $N(t)$ inside corrals that are infrequently crossed (static corral case) or for gates that open infrequently with short duration (Leitner et al., 2000), but that invoking this approximation to describe the variance and higher moments of the population is harder to justify.

We denote the rate constants for protein influx and loss as λ and μ, respectively. μ may be obtained analytically for simple corral geometries or numerically from simulation in general (Saxton, 1995). The average number of proteins inside the corral at long times (when equilibrium with the sea has been reached) is denoted by $\langle N\rangle$ and together with μ sets the rate $\lambda = \mu\langle N\rangle$ by detailed balance (Kubo et al., 1998). Given that the sea of proteins is in constant equilibrium and we have assumed rate processes for the escape/entrance of proteins from/to the corral, our system is completely specified by the number of proteins inside the corral as a function of time. Denoting the probability that there are n proteins in a corral at time t as $P_n(t)$, we arrive at the set of equations

$$\dot{P}_0(t) = -\lambda P_0(t) + \mu P_1(t)$$

$$\dot{P}_n(t) = -(\lambda + n\mu)P_n(t) + \lambda P_{n-1}(t) + (n+1)\mu P_{n+1}(t). \tag{A1}$$

Consider the generating function,

$$P(s, t) \equiv \sum_{n=0} P_n(t)s^n. \tag{A2}$$

It is easily verified that Eq. A1 implies that the generating function obeys

$$\frac{\partial P}{\partial t} = (1 - s)\left\{-\lambda P + \mu \frac{\partial P}{\partial s}\right\}, \tag{A3}$$

which has the solution (Feller, 1968)

$$P(s, t) = \exp(-\langle N\rangle(1 - s)(1 - e^{-\mu t}))(1 - (1 - s)e^{-\mu t})^{N(0)} \tag{A4}$$

for the initial condition $\{P_{N(0)}(0) = 1, P_{n\neq N(0)}(0) = 0\}$. For simplicity we have assumed that the corral begins with a specific number of proteins; this restriction is easily relaxed by averaging our results over an initial distribution of protein occupations. Because the average population and average square population are obtained from the generating function by (Feller,

1968)

$$\overline{N(t)} = \left.\frac{\partial P}{\partial s}\right|_{s=1}$$

$$\overline{N(t)^2} = \left.\frac{\partial^2 P}{\partial s^2}\right|_{s=1} + \left.\frac{\partial P}{\partial s}\right|_{s=1}, \qquad \text{(A5)}$$

we obtain

$$\overline{N(t)} = (N(0) - \langle N\rangle)e^{-\mu t} + \langle N\rangle$$

$$\overline{N(t)^2} - \overline{N(t)}^2 = N(0)e^{-\mu t}(1 - e^{-\mu t}) + \langle N\rangle(1 - e^{-\mu t}) \qquad \text{(A6)}$$

for the population and variance.

Dynamic corral

Consider now a dynamically gated corral. Although we were concerned primarily with open-closed gating in the body of this paper, we present here a derivation for a slightly more general situation, namely that the corral has a boundary that is stochastically fluctuating in such a way as to give rise to time dependence of the rate constants μ and λ discussed above. In the open-closed model this simply corresponds to rate constants that assume only two values (zero and the free diffusion values) as time evolves. This generalization to time-dependent rate constants trivially complicates the set of coupled Eqs. A1 to

$$\dot{P}_0(t) = -\lambda(t)P_0(t) + \mu(t)P_1(t)$$

$$\dot{P}_n(t) = -(\lambda(t) + n\mu(t))P_n(t) + \lambda(t)P_{n-1}(t) + (n+1)\mu(t)P_{n+1}(t), \qquad \text{(A7)}$$

where the time dependence of $\mu(t)$ and $\lambda(t)$ has been explicitly included. These equations lead to an analog of Eq. A3, with μ and λ replaced by their time-dependent generalizations. The generating function that solves this equation is given by

$$P(s,t) = \exp(-\langle N\rangle(1-s)(1 - e^{-\int_0 \mu(\tau)d\tau})) \cdot(1-(1-s)e^{-\int_0 \mu(\tau)d\tau})^{N(0)}. \qquad \text{(A8)}$$

Utilizing the differentiation formulae (Eq. A5), we are led to expressions for the average population and average square population for a given stochastic trajectory of the gate defined by a set temporal dependence of $\mu(t)$ and $\lambda(t)$:

$$\overline{N(t)}_{traj.} = (N(0) - \langle N\rangle)e^{-\int_0 \mu(\tau)d\tau} + \langle N\rangle \qquad \text{(A9)}$$

$$\overline{N(t)^2}_{traj.} = N(0)(e^{-\int_0 \mu(\tau)d\tau} - e^{-2\int_0 \mu(\tau)d\tau}) + \langle N\rangle(1-e^{-\int_0 \mu(\tau)d\tau}) + \langle N\rangle^2 + (N(0)-\langle N\rangle)^2 e^{-2\int_0 \mu(\tau)d\tau} + 2\langle N\rangle(N(0)-\langle N\rangle)e^{-\int_0 \mu(\tau)d\tau}.$$

The averaging $(\overline{(\ldots)}_{traj.})$ in the above equations reflects only averaging over proteins entering and leaving the corral for a given temporal behavior of the gate. In practice we need to define an average $(\overline{(\ldots)})$ that further averages the above formulae over all possible stochastic trajectories for the gate. Inspection of the above formulae reveals that arriving at a solution for such a trajectory-averaged result requires computation of terms resembling

$$\langle e^{-\int_0 \mu(\tau)d\tau}\rangle_T, \qquad \text{(A10)}$$

where $\langle\ldots\rangle_T$ represents an average over all possible stochastic trajectories for the gate. In general it is not a simple matter to compute this quantity, but for gating mechanisms with sufficiently simple stochastic properties there do exist analytical solutions (Zwanzig, 1990). Our focus here will be on solutions when the gate may occupy a finite number of states and there is random Markovian hopping between these gating states. In this case, averages such as Eq. A10 closely resemble expressions familiar to chemical physicists dealing with line broadening in condensed phases, and the solutions are well known (Kubo, 1962).

For simplicity, consider a two-state gating system with protein loss rates μ_1 and μ_2 in each of the two states and transition rates between the two states given by $W_{1\to2}$ and $W_{2\to1}$. (Because the equilibrium value of N is $\langle N\rangle$ for both of these states we also necessarily have two different protein influx rates $\lambda_1 = \langle N\rangle\mu_1$ and $\lambda_2 = \langle N\rangle\mu_2$.) The expression for Eq. A10 is then given by (Kubo, 1962)

$$\langle e^{-\int_0 \mu(\tau)d\tau}\rangle_T = (1,1)\cdot\exp\left[t\begin{pmatrix} -\mu_1 - W_{1\to2} & W_{2\to1} \\ W_{1\to2} & -\mu_2 - W_{2\to1}\end{pmatrix}\right] \cdot\begin{pmatrix}\dfrac{W_{2\to1}}{(W_{1\to2}+W_{2\to1})} \\ \dfrac{W_{1\to2}}{(W_{1\to2}+W_{2\to1})}\end{pmatrix}. \qquad \text{(A11)}$$

Generalizing the above expression to more than two gating states should be transparent. The exponentiated matrix becomes $N \times N$ instead of 2×2 and is filled with the various transition probabilities between states. Along the diagonal there will be the addition of $-\mu_i's$ to the sum of the negative rates to the other gating states. The column vector becomes filled with the probabilities that the gate will be found in a given state at equilibrium, and the row vector becomes a $1 \times N$ vector of ones.

Our final expressions for the average population and variance are most easily written in terms of the functions

$$\mathcal{W}_1(t) \equiv \langle e^{-\int_0 \mu(\tau)d\tau}\rangle_T$$

$$\mathcal{W}_2(t) \equiv \langle e^{-2\int_0 \mu(\tau)d\tau}\rangle_T, \qquad \text{(A12)}$$

where it is understood that the $\mathcal{W}(t)'s$ depend upon the $\mu_i's$ and $W'_{i\to j}s$ for the system in question, as dictated by Eq. A11 for $\mathcal{W}_1(t)$ and a modified form of Eq. A11, where each μ_i is replaced with $2\mu_i$ for $\mathcal{W}_2(t)$. The final results for the average population and variance are given in Eq. 5 of the text. These equations simplify for the case of an empty bath (i.e., $\langle N\rangle = 0$) or a corral that begins empty (i.e., $N(0) = 0$). We have concentrated on these situations in the text.

We thank Paul Wiseman for stimulating discussions.

This material is based upon work supported in part by the National Science Foundation under a fellowship grant awarded to FLHB in 1999.

REFERENCES

Berg, H. C., and E. M. Purcell. 1977. Physics of chemoreception. *Biophys. J.* 20:193–219.

Boal, D. H. 1994. Computer simulation of a model network for the erythrocyte cytoskeleton. *Biophys. J.* 67:521–529.

Boal, D. H., and S. K. Boey. 1995. Barrier-free paths of directed protein motion in the erythrocyte plasma membrane. *Biophys. J.* 69:372–379.

Cherry, R. J. 1979. Rotational and lateral diffusion of membrane proteins. *Biochim. Biophys. Acta.* 559:289–327.

Corbett, J. D., P. Agre, J. Palek, and D. E. Golan. 1994. Differential control of band 3 lateral and rotational mobility in intact red cells. *J. Clin. Invest.* 94:683–688.

Edidin, M. 1990. Molecular associations and membrane domains. *Curr. Top. Membr. Transp.* 36:81–96.

Edidin, M., S. C. Kuo, and M. P. Sheetz. 1991. Lateral movements of membrane glycoproteins restricted by dynamic cytoplasmic barriers. *Science.* 254:1379–1382.

Feller, W. 1968. An Introduction to Probability Theory and Its Applications, Vol. 1, 3rd Ed. John Wiley and Sons, New York.

Fleming, T. P. 1987. Trapped by a skeleton—the maintenance of epithelial membrane dynamics. *Bioassays.* 7:179–181.

Gennis, R. B. 1989. Biomembranes: Molecular Structure and Function. Springer-Verlag, Berlin.

Giancotti, F. G., and E. Ruoslahti. 1999. Integrin signaling. *Science.* 285:1028–1032.

Hänggi, P., P. Talkner, and M. Borkovec. 1990. Reaction-rate theory: fifty years after Kramers. *Rev. Mod. Phys.* 62:251–341.

Jacobson, K., E. D. Sheets, and R. Simson. 1995. Revisiting the fluid mosaic model of membranes. *Science.* 268:1441–1442.

Koppel, D. E., M. P. Sheetz, and M. Schindler. 1981. Matrix control of protein diffusion in biological membranes. *Proc. Natl. Acad. Sci. USA.* 78:3576–3580.

Kubo, R. 1962. Stochastic theory of line-shape. *In* Fluctuation, Relaxation and Resonance in Magnetic Systems. D. TerHaar, editor. Oliver and Boyd, Edinburgh. 23–68.

Kubo, R., M. Toda, and N. Hashitsume. 1998. Statistical Physics II: Nonequilibrium Statistical Mechanics, 2nd Ed. Springer-Verlag, Berlin.

Kusumi, A., and Y. Sako. 1996. Cell surface organization by the membrane skeleton. *Curr. Opin. Cell Biol.* 8:566–574.

Kusumi, A., Y. Sako, T. Fujiwara, and M. Tomishige. 1998. Application of laser tweezers to studies of the fences and tethers of the membrane skeleton that regulate the movements of plasma membrane proteins. *Methods Cell Biol.* 55:174–194.

Lauffenburger, D. A., and J. J. Linderman. 1993. Receptors: Models for Binding, Trafficking and Signaling. Oxford University Press, New York.

Leitner, D. M., F. L. H. Brown, and K. R. Wilson. 2000. Regulation of protein mobility in cell membranes: a dynamic corral model. *Biophys. J.* 78:125–135.

Levi, B. G. 1999. Progress made in near-field imaging with light from a sharp tip. *Phys. Today.* 52:18–20.

Qian, H., M. P. Sheetz, and E. L. Elson. 1991. Single particle tracking: analysis of diffusion and flow in two-dimensional systems. *Biophys. J.* 60:910–921.

Sako, Y., and A. Kusumi. 1995. Barriers for lateral diffusion of transferrin receptor in the plasma membrane as characterized by receptor dragging by laser tweezers: fence versus tether. *J. Cell Biol.* 129:1559–1574.

Saxton, M. J. 1989. The spectrin network as a barrier to lateral diffusion in erythrocytes: a percolation analysis. *Biophys. J.* 55:21–28.

Saxton, M. J. 1990a. The membrane skeleton of erythrocytes: a percolation model. *Biophys. J.* 57:1167–1177.

Saxton, M. J. 1990b. The membrane skeleton of erythrocytes: models of its effect on lateral diffusion. *Int. J. Biochem.* 22:801–809.

Saxton, M. J. 1995. Single-particle tracking: effects of corrals. *Biophys. J.* 69:389–398.

Saxton, M. J., and K. Jacobson. 1997. Single particle tracking: applications to membrane dynamics. *Annu. Rev. Biophys. Biomol. Struct.* 26: 373–399.

Schindler, M., D. E. Koppel, and M. P. Sheetz. 1980. Modulation of protein lateral mobility by polyphosphates and polyamines. *Proc. Natl. Acad. Sci. USA.* 77:1457–1461.

Sheetz, M. P. 1983. Membrane skeletal dynamics: role in modulation of red blood cell deformability, mobility of transmembrane proteins, and shape. *Semin. Hematol.* 20:175–188.

Sheetz, M. P., M. Schindler, and D. E. Koppel. 1980. The lateral mobility of integral membrane proteins is increased in spherocytic erythrocytes. *Nature.* 285:510–512.

Singer, S. J., and G. L. Nicolson. 1972. The fluid mosaic model of the structure of cell membranes. *Science.* 175:720–731.

Tomishige, M. 1997. Regulation mechanism of the lateral diffusion of band 3 in erythrocyte membranes: corralling and binding effects of the membrane skeleton. Ph.D. thesis. University of Tokyo.

Tomishige, M., and A. Kusumi. 1999. Regulation of band 3 diffusion by dissociation-association equilibrium of the erythrocyte membrane skeleton. *Biophys. J.* 76:A390.

Tomishige, M., Y. Sako, and A. Kusumi. 1998. Regulation mechanism of the lateral diffusion of band 3 in erythrocyte membranes by the membrane skeleton. *J. Cell Biol.* 142:989–1000.

Tsuji, A., K. Kawasaki, S. Ohnishi, H. Merkle, and A. Kusumi. 1988. Regulation of band 3 mobilities in erythrocyte ghost membranes by protein association and cytoskeletal meshwork. *Biochemistry.* 27: 7447–7452.

Tsuji, A., and S. Ohnishi. 1986. Restriction of the lateral motion of band 3 in the erythrocyte membrane by the cytoskeletal network: dependence on spectrin association state. *Biochemistry.* 25:6133–6139.

van Kampen, N. G. 1992. Stochastic Processes in Chemistry and Physics, 2nd Ed. North-Holland, Amsterdam.

Wang, J., and P. Wolynes. 1995. Intermittency of single molecule reaction dynamics in fluctuating environments. *Phys. Rev. Lett.* 74:4317–4320.

Williams, W. J., E. Beutler, A. J. Erslev, and M. A. Lichtman. 1990. Hematology, 4th Ed. McGraw-Hill, New York.

Winckler, B., P. Forscher, and I. Mellman. 1999. A diffusion barrier maintains distribution of membrane proteins in polarized neurons. *Nature.* 397:698–701.

Zwanzig, R. 1990. Rate processes with dynamical disorder. *Accounts Chem. Res.* 23:148–152.